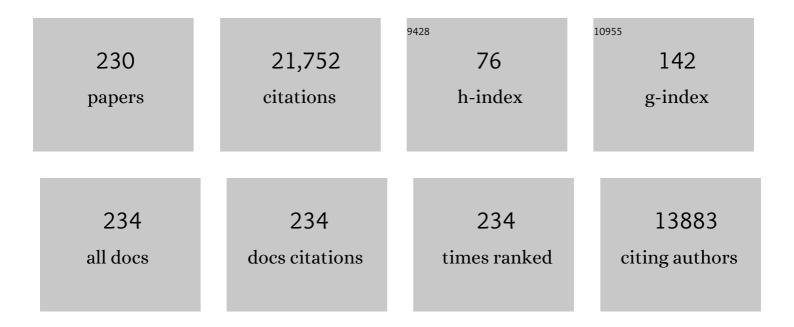
List of Publications by Year in descending order

Source: https://exaly.com/author-pdf/7121524/publications.pdf Version: 2024-02-01



#	Article	IF	CITATIONS
1	Clinical recommendations for cardiovascular magnetic resonance mapping of T1, T2, T2* and extracellular volume: A consensus statement by the Society for Cardiovascular Magnetic Resonance (SCMR) endorsed by the European Association for Cardiovascular Imaging (EACVI). Journal of Cardiovascular Magnetic Resonance, 2017, 19, 75.	1.6	1,074
2	Phase-sensitive inversion recovery for detecting myocardial infarction using gadolinium-delayed hyperenhancement. Magnetic Resonance in Medicine, 2002, 47, 372-383.	1.9	941
3	Myocardial T1 mapping and extracellular volume quantification: a Society for Cardiovascular Magnetic Resonance (SCMR) and CMR Working Group of the European Society of Cardiology consensus statement. Journal of Cardiovascular Magnetic Resonance, 2013, 15, 92.	1.6	864
4	Adaptive sensitivity encoding incorporating temporal filtering (TSENSE). Magnetic Resonance in Medicine, 2001, 45, 846-852.	1.9	764
5	Dynamic autocalibrated parallel imaging using temporal GRAPPA (TGRAPPA). Magnetic Resonance in Medicine, 2005, 53, 981-985.	1.9	611
6	T1-mapping in the heart: accuracy and precision. Journal of Cardiovascular Magnetic Resonance, 2014, 16, 2.	1.6	551
7	ACUT ₂ E TSEâ€SSFP: A hybrid method for T2â€weighted imaging of edema in the heart. Magnetic Resonance in Medicine, 2008, 59, 229-235.	1.9	536
8	Extracellular volume imaging by magnetic resonance imaging provides insights into overt and sub-clinical myocardial pathology. European Heart Journal, 2012, 33, 1268-1278.	1.0	482
9	Motion corrected freeâ€breathing delayedâ€enhancement imaging of myocardial infarction using nonrigid registration. Journal of Magnetic Resonance Imaging, 2007, 26, 184-190.	1.9	470
10	Image reconstruction in SNR units: A general method for SNR measurement. Magnetic Resonance in Medicine, 2005, 54, 1439-1447.	1.9	443
11	Prognostic Value of Late Gadolinium Enhancement Cardiovascular Magnetic Resonance in Cardiac Amyloidosis. Circulation, 2015, 132, 1570-1579.	1.6	442
12	Association Between Extracellular Matrix Expansion Quantified by Cardiovascular Magnetic Resonance and Short-Term Mortality. Circulation, 2012, 126, 1206-1216.	1.6	422
13	MultiContrast Delayed Enhancement (MCODE) improves detection of subendocardial myocardial infarction by late gadolinium enhancement cardiovascular magnetic resonance: a clinical validation study. Journal of Cardiovascular Magnetic Resonance, 2012, 14, 86.	1.6	420
14	Improved cine displacement-encoded MRI using balanced steady-state free precession and time-adaptive sensitivity encoding parallel imaging at 3 T. NMR in Biomedicine, 2007, 20, 591-601.	1.6	419
15	Extracellular volume fraction mapping in the myocardium, part 1: evaluation of an automated method. Journal of Cardiovascular Magnetic Resonance, 2012, 14, 60.	1.6	323
16	Myocardial extracellular volume fraction quantified by cardiovascular magnetic resonance is increased in diabetes and associated with mortality and incident heart failure admission. European Heart Journal, 2014, 35, 657-664.	1.0	297
17	Gadolinium delayed enhancement cardiovascular magnetic resonance correlates with clinical measures of myocardial infarction. Journal of the American College of Cardiology, 2004, 43, 2253-2259.	1.2	292
18	Magnetic Resonance in TransthyretinÂCardiac Amyloidosis. Journal of the American College of Cardiology, 2017, 70, 466-477.	1.2	290

#	Article	IF	CITATIONS
19	Myocardial Edema as Detected by Pre-Contrast T1 and T2 CMR Delineates Area at Risk Associated With Acute Myocardial Infarction. JACC: Cardiovascular Imaging, 2012, 5, 596-603.	2.3	283
20	Patterns of myocardial injury in recovered troponin-positive COVID-19 patients assessed by cardiovascular magnetic resonance. European Heart Journal, 2021, 42, 1866-1878.	1.0	274
21	Reverse Myocardial Remodeling FollowingÂValve Replacement in PatientsÂWith Aortic Stenosis. Journal of the American College of Cardiology, 2018, 71, 860-871.	1.2	266
22	Accuracy, Precision, and Reproducibility of Four T1 Mapping Sequences: A Head-to-Head Comparison of MOLLI, ShMOLLI, SASHA, and SAPPHIRE. Radiology, 2014, 272, 683-689.	3.6	255
23	Prevalence and Prognosis of Unrecognized Myocardial Infarction Determined by Cardiac Magnetic Resonance in Older Adults. JAMA - Journal of the American Medical Association, 2012, 308, 890.	3.8	234
24	Opportunities in Interventional and Diagnostic Imaging by Using High-Performance Low-Field-Strength MRI. Radiology, 2019, 293, 384-393.	3.6	224
25	Extracellular volume fraction mapping in the myocardium, part 2: initial clinical experience. Journal of Cardiovascular Magnetic Resonance, 2012, 14, 61.	1.6	223
26	T2-prepared SSFP improves diagnostic confidence in edema imaging in acute myocardial infarction compared to turbo spin echo. Magnetic Resonance in Medicine, 2007, 57, 891-897.	1.9	219
27	Dynamic Changes of Edema and Late Gadolinium Enhancement After Acute Myocardial Infarction and Their Relationship to Functional Recovery and Salvage Index. Circulation: Cardiovascular Imaging, 2011, 4, 228-236.	1.3	214
28	Myocardial extravascular extracellular volume fraction measurement by gadolinium cardiovascular magnetic resonance in humans: slow infusion versus bolus. Journal of Cardiovascular Magnetic Resonance, 2011, 13, 16.	1.6	198
29	Motion correction for myocardial T1 mapping using image registration with synthetic image estimation. Magnetic Resonance in Medicine, 2012, 67, 1644-1655.	1.9	187
30	Myocardial perfusion cardiovascular magnetic resonance: optimized dual sequence and reconstruction for quantification. Journal of Cardiovascular Magnetic Resonance, 2016, 19, 43.	1.6	185
31	Myocardial Fibrosis Quantified by Extracellular Volume Is Associated With Subsequent Hospitalization for Heart Failure, Death, or Both Across the Spectrum of Ejection Fraction and Heart Failure Stage. Journal of the American Heart Association, 2015, 4, .	1.6	174
32	Preliminary investigation of respiratory self-gating for free-breathing segmented cine MRI. Magnetic Resonance in Medicine, 2005, 53, 159-168.	1.9	172
33	Native T1 and Extracellular Volume inÂTransthyretin Amyloidosis. JACC: Cardiovascular Imaging, 2019, 12, 810-819.	2.3	172
34	Assessment of Myocardial Microstructural Dynamics by InÂVivo Diffusion Tensor Cardiac Magnetic Resonance. Journal of the American College of Cardiology, 2017, 69, 661-676.	1.2	171
35	Temporal Relation Between Myocardial Fibrosis and Heart Failure With Preserved Ejection Fraction. JAMA Cardiology, 2017, 2, 995.	3.0	164
36	Late Gadolinium-Enhancement Cardiac Magnetic Resonance Identifies Postinfarction Myocardial Fibrosis and the Border Zone at the Near Cellular Level in Ex Vivo Rat Heart. Circulation: Cardiovascular Imaging, 2010, 3, 743-752.	1.3	156

#	Article	IF	CITATIONS
37	Quantitative myocardial infarction on delayed enhancement MRI. Part I: Animal validation of an automated feature analysis and combined thresholding infarct sizing algorithm. Journal of Magnetic Resonance Imaging, 2006, 23, 298-308.	1.9	154
38	Reproducibility of native myocardial T1 mapping in the assessment of Fabry disease and its role in early detection of cardiac involvement by cardiovascular magnetic resonance. Journal of Cardiovascular Magnetic Resonance, 2014, 16, 99.	1.6	154
39	Myocardial Edema and Prognosis inÂAmyloidosis. Journal of the American College of Cardiology, 2018, 71, 2919-2931.	1.2	145
40	Myocardial T1 and extracellular volume fraction mapping at 3 tesla. Journal of Cardiovascular Magnetic Resonance, 2011, 13, 75.	1.6	144
41	T1 and extracellular volume mapping in the heart: estimation of error maps and the influence of noise on precision. Journal of Cardiovascular Magnetic Resonance, 2013, 15, 56.	1.6	143
42	Application of sensitivity-encoded echo-planar imaging for blood oxygen level-dependent functional brain imaging. Magnetic Resonance in Medicine, 2002, 48, 1011-1020.	1.9	142
43	Automated Pixel-Wise Quantitative Myocardial Perfusion Mapping by CMRÂtoÂDetect Obstructive Coronary Artery Disease and Coronary Microvascular Dysfunction. JACC: Cardiovascular Imaging, 2019, 12, 1958-1969.	2.3	140
44	Noncontrast myocardial <i>T</i> ₁ mapping using cardiovascular magnetic resonance for iron overload. Journal of Magnetic Resonance Imaging, 2015, 41, 1505-1511.	1.9	139
45	Cardiac imaging techniques for physicians: Late enhancement. Journal of Magnetic Resonance Imaging, 2012, 36, 529-542.	1.9	136
46	A medical device-grade T1 and ECV phantom for global T1 mapping quality assurance—the T1 Mapping and ECV Standardization in cardiovascular magnetic resonance (T1MES) program. Journal of Cardiovascular Magnetic Resonance, 2016, 18, 58.	1.6	134
47	Quantitative myocardial perfusion analysis with a dual-bolus contrast-enhanced first-pass MRI technique in humans. Journal of Magnetic Resonance Imaging, 2006, 23, 315-322.	1.9	130
48	Automatic Measurement of the MyocardialÂInterstitium. JACC: Cardiovascular Imaging, 2016, 9, 54-63.	2.3	127
49	Imaging Sequences for First Pass Perfusion - A Review. Journal of Cardiovascular Magnetic Resonance, 2007, 9, 525-537.	1.6	126
50	COVID-19. Circulation, 2020, 142, 1120-1122.	1.6	126
51	Noncontrast Magnetic Resonance for theÂDiagnosis of Cardiac Amyloidosis. JACC: Cardiovascular Imaging, 2020, 13, 69-80.	2.3	125
52	A Quantitative Pixel-Wise Measurement of Myocardial Blood Flow by Contrast-Enhanced First-Pass CMR Perfusion Imaging. JACC: Cardiovascular Imaging, 2012, 5, 154-166.	2.3	120
53	Residual Myocardial Iron Following Intramyocardial Hemorrhage During the Convalescent Phase of Reperfused ST-Segment–Elevation Myocardial Infarction and Adverse Left Ventricular Remodeling. Circulation: Cardiovascular Imaging, 2016, 9, .	1.3	120
54	Adiabatic inversion pulses for myocardial T1 mapping. Magnetic Resonance in Medicine, 2014, 71, 1428-1434.	1.9	119

#	Article	IF	CITATIONS
55	Chemical shift–based water/fat separation: A comparison of signal models. Magnetic Resonance in Medicine, 2010, 64, 811-822.	1.9	116
56	Motion-corrected free-breathing delayed enhancement imaging of myocardial infarction. Magnetic Resonance in Medicine, 2005, 53, 194-200.	1.9	115
57	Multiecho dixon fat and water separation method for detecting fibrofatty infiltration in the myocardium. Magnetic Resonance in Medicine, 2009, 61, 215-221.	1.9	115
58	Magnetic Resonance Imaging Delineates the Ischemic Area at Risk and Myocardial Salvage in Patients With Acute Myocardial Infarction. Circulation: Cardiovascular Imaging, 2010, 3, 527-535.	1.3	114
59	Reduction in CMR Derived Extracellular Volume With Patisiran Indicates Cardiac Amyloid Regression. JACC: Cardiovascular Imaging, 2021, 14, 189-199.	2.3	113
60	Prospective Case-Control Study of Cardiovascular Abnormalities 6ÂMonthsÂFollowing Mild COVID-19 inÂHealthcare Workers. JACC: Cardiovascular Imaging, 2021, 14, 2155-2166.	2.3	111
61	Temporal dynamics of the BOLD fMRI impulse response. NeuroImage, 2005, 24, 667-677.	2.1	110
62	Fully quantitative cardiovascular magnetic resonance myocardial perfusion ready for clinical use: a comparison between cardiovascular magnetic resonance imaging and positron emission tomography. Journal of Cardiovascular Magnetic Resonance, 2016, 19, 78.	1.6	110
63	Assessment of regional systolic and diastolic dysfunction in familial hypertrophic cardiomyopathy using MR tagging. Magnetic Resonance in Medicine, 2003, 50, 638-642.	1.9	102
64	Detection and Monitoring of Acute Myocarditis Applying Quantitative Cardiovascular Magnetic Resonance. Circulation: Cardiovascular Imaging, 2017, 10, .	1.3	100
65	The Prognostic Significance of Quantitative Myocardial Perfusion: An Artificial Intelligence Based Approach Using Perfusion Mapping. Circulation, 2020, 141, 1282-1291.	1.6	100
66	Diagnostic Accuracy of Stress Perfusion CMR in Comparison With Quantitative Coronary Angiography. JACC: Cardiovascular Imaging, 2014, 7, 14-22.	2.3	97
67	Phaseâ€sensitive inversion recovery for myocardial <i>T</i> ₁ mapping with motion correction and parametric fitting. Magnetic Resonance in Medicine, 2013, 69, 1408-1420.	1.9	90
68	Modular 32-channel transceiver coil array for cardiac MRI at 7.0T. Magnetic Resonance in Medicine, 2014, 72, 276-290.	1.9	90
69	Real-time MRI-guided right heart catheterization in adults using passive catheters. European Heart Journal, 2013, 34, 380-389.	1.0	88
70	Real-time accelerated interactive MRI with adaptive TSENSE and UNFOLD. Magnetic Resonance in Medicine, 2003, 50, 315-321.	1.9	87
71	High spatial and temporal resolution cardiac cine MRI from retrospective reconstruction of data acquired in real time using motion correction and resorting. Magnetic Resonance in Medicine, 2009, 62, 1557-1564.	1.9	87
72	Influence of Off-resonance in myocardial T1-mapping using SSFP based MOLLI method. Journal of Cardiovascular Magnetic Resonance, 2013, 15, 63.	1.6	85

#	Article	IF	CITATIONS
73	Virtual coil concept for improved parallel MRI employing conjugate symmetric signals. Magnetic Resonance in Medicine, 2009, 61, 93-102.	1.9	83
74	Characterization of myocardial T1-mapping bias caused by intramyocardial fat in inversion recovery and saturation recovery techniques. Journal of Cardiovascular Magnetic Resonance, 2015, 17, 33.	1.6	80
75	Retrospective reconstruction of high temporal resolution cine images from realâ€ŧime MRI using iterative motion correction. Magnetic Resonance in Medicine, 2012, 68, 741-750.	1.9	78
76	Myocardial native T1 and extracellular volume with healthy ageing and gender. European Heart Journal Cardiovascular Imaging, 2018, 19, 615-621.	0.5	78
77	Quantitative myocardial infarction on delayed enhancement MRI. Part II: Clinical application of an automated feature analysis and combined thresholding infarct sizing algorithm. Journal of Magnetic Resonance Imaging, 2006, 23, 309-314.	1.9	77
78	Twoâ€Dimensional sixteen channel transmit/receive coil array for cardiac MRI at 7.0 T: Design, evaluation, and application. Journal of Magnetic Resonance Imaging, 2012, 36, 847-857.	1.9	76
79	High spatial and temporal resolution retrospective cine cardiovascular magnetic resonance from shortened free breathing real-time acquisitions. Journal of Cardiovascular Magnetic Resonance, 2013, 15, 102.	1.6	75
80	Myocardial Fat Imaging. Current Cardiovascular Imaging Reports, 2010, 3, 83-91.	0.4	72
81	Hunting for neuronal currents: absence of rapid MRI signal changes during visual-evoked response. NeuroImage, 2004, 23, 1059-1067.	2.1	71
82	Comparison of three multichannel transmit/receive radiofrequency coil configurations for anatomic and functional cardiac MRI at 7.0T: implications for clinical imaging. European Radiology, 2012, 22, 2211-2220.	2.3	68
83	Extracellular Volume Associates WithÂOutcomes More Strongly Than Native or Post-Contrast Myocardial T1. JACC: Cardiovascular Imaging, 2020, 13, 44-54.	2.3	68
84	Semiautomated Segmentation of Myocardial Contours for Fast Strain Analysis in Cine Displacement-Encoded MRI. IEEE Transactions on Medical Imaging, 2008, 27, 1084-1094.	5.4	65
85	Fully automatic, retrospective enhancement of realâ€time acquired cardiac cine MR images using imageâ€based navigators and respiratory motionâ€corrected averaging. Magnetic Resonance in Medicine, 2008, 59, 771-778.	1.9	64
86	Dark blood late enhancement imaging. Journal of Cardiovascular Magnetic Resonance, 2016, 18, 77.	1.6	64
87	Free-Breathing, Motion-Corrected Late Gadolinium Enhancement Is Robust and Extends Risk Stratification to Vulnerable Patients. Circulation: Cardiovascular Imaging, 2013, 6, 423-432.	1.3	59
88	Bright-Blood T ₂ -Weighted MRI Has High Diagnostic Accuracy for Myocardial Hemorrhage in Myocardial Infarction. Circulation: Cardiovascular Imaging, 2011, 4, 738-745.	1.3	57
89	Nonlinear myocardial signal intensity correction improves quantification of contrastâ€enhanced firstâ€pass MR perfusion in humans. Journal of Magnetic Resonance Imaging, 2008, 27, 793-801.	1.9	56
90	Fully automated, inline quantification of myocardial blood flow with cardiovascular magnetic resonance: repeatability of measurements in healthy subjects. Journal of Cardiovascular Magnetic Resonance, 2018, 20, 48.	1.6	54

#	Article	IF	CITATIONS
91	Native T1 values identify myocardial changes and stratify disease severity in patients with Duchenne muscular dystrophy. Journal of Cardiovascular Magnetic Resonance, 2016, 18, 72.	1.6	51
92	Distributed MRI reconstruction using gadgetron-based cloud computing. Magnetic Resonance in Medicine, 2015, 73, 1015-1025.	1.9	50
93	Automatic motion compensation of free breathing acquired myocardial perfusion data by using independent component analysis. Medical Image Analysis, 2012, 16, 1015-1028.	7.0	48
94	Contrast-free detection of myocardial fibrosis in hypertrophic cardiomyopathy patients with diffusion-weighted cardiovascular magnetic resonance. Journal of Cardiovascular Magnetic Resonance, 2015, 17, 107.	1.6	48
95	Multicontrast delayed enhancement provides improved contrast between myocardial infarction and blood pool. Journal of Magnetic Resonance Imaging, 2005, 22, 605-613.	1.9	46
96	Design, evaluation and application of an eight channel transmit/receive coil array for cardiac MRI at 7.0T. European Journal of Radiology, 2013, 82, 752-759.	1.2	46
97	Automated Extracellular Volume Fraction Mapping Provides Insights Into the Pathophysiology of Left Ventricular Remodeling Post–Reperfused STâ€Elevation Myocardial Infarction. Journal of the American Heart Association, 2016, 5, .	1.6	46
98	Low b-Value Diffusion-Weighted Cardiac Magnetic Resonance Imaging. Investigative Radiology, 2011, 46, 751-758.	3.5	44
99	Image reconstruction: An overview for clinicians. Journal of Magnetic Resonance Imaging, 2015, 41, 573-585.	1.9	43
100	Optimized saturation recovery protocols for T1-mapping in the heart: influence of sampling strategies on precision. Journal of Cardiovascular Magnetic Resonance, 2014, 16, 55.	1.6	42
101	Extracellular Volume and Global Longitudinal Strain Both Associate WithÂOutcomes But Correlate Minimally. JACC: Cardiovascular Imaging, 2020, 13, 2343-2354.	2.3	42
102	Cardiac Involvement in Myotonic Dystrophy Type 2 Patients With Preserved Ejection Fraction. Circulation: Cardiovascular Imaging, 2016, 9, .	1.3	41
103	CMR fluoroscopy right heart catheterization for cardiac output and pulmonary vascular resistance: results in 102 patients. Journal of Cardiovascular Magnetic Resonance, 2016, 19, 54.	1.6	41
104	Quantification of both the area-at-risk and acute myocardial infarct size in ST-segment elevation myocardial infarction using T1-mapping. Journal of Cardiovascular Magnetic Resonance, 2016, 19, 57.	1.6	41
105	Chost artifact cancellation using phased array processing. Magnetic Resonance in Medicine, 2001, 46, 335-343.	1.9	40
106	Multishot EPI-SSFP in the heart. Magnetic Resonance in Medicine, 2002, 47, 655-664.	1.9	40
107	Myocardial Damage Detected by Late Gadolinium Enhancement Cardiovascular Magnetic Resonance Is Associated With Subsequent Hospitalization for Heart Failure. Journal of the American Heart Association, 2013, 2, e000416.	1.6	39
108	Females have higher myocardial perfusion, blood volume and extracellular volume compared to males – an adenosine stress cardiovascular magnetic resonance study. Scientific Reports, 2020, 10, 10380.	1.6	39

#	Article	IF	CITATIONS
109	Real-time, Interactive MRI for Cardiovascular Interventions1. Academic Radiology, 2005, 12, 1121-1127.	1.3	36
110	Prospective comparison of novel dark blood late gadolinium enhancement with conventional bright blood imaging for the detection of scar. Journal of Cardiovascular Magnetic Resonance, 2016, 19, 91.	1.6	36
111	Empagliflozin Treatment Is Associated With Improvements in Cardiac Energetics and Function and Reductions in Myocardial Cellular Volume in Patients With Type 2 Diabetes. Diabetes, 2021, 70, 2810-2822.	0.3	36
112	MIA - A free and open source software for gray scale medical image analysis. Source Code for Biology and Medicine, 2013, 8, 20.	1.7	35
113	Distinction of salvaged and infarcted myocardium within the ischaemic area-at-risk with T2 mapping. European Heart Journal Cardiovascular Imaging, 2014, 15, 1048-1053.	0.5	35
114	Myocardial T2* mapping: influence of noise on accuracy and precision. Journal of Cardiovascular Magnetic Resonance, 2015, 17, 7.	1.6	35
115	Quantitative myocardial perfusion in coronary artery disease: A perfusion mapping study. Journal of Magnetic Resonance Imaging, 2019, 50, 756-762.	1.9	35
116	Variability of myocardial perfusion dark rim Gibbs artifacts due to sub-pixel shifts. Journal of Cardiovascular Magnetic Resonance, 2009, 11, 17.	1.6	34
117	Integration of cardiac and respiratory motion into MRI roadmaps fused with xâ€ray. Medical Physics, 2013, 40, 032302.	1.6	33
118	Simultaneous multislice imaging for native myocardial T ₁ mapping: Improved spatial coverage in a single breath-hold. Magnetic Resonance in Medicine, 2017, 78, 462-471.	1.9	32
119	Quantitative Myocardial Perfusion in Fabry Disease. Circulation: Cardiovascular Imaging, 2019, 12, e008872.	1.3	32
120	Automated Inline Analysis of Myocardial Perfusion MRI with Deep Learning. Radiology: Artificial Intelligence, 2020, 2, e200009.	3.0	32
121	Phased array ghost elimination. NMR in Biomedicine, 2006, 19, 352-361.	1.6	31
122	Saturation pulse design for quantitative myocardial T1 mapping. Journal of Cardiovascular Magnetic Resonance, 2015, 17, 84.	1.6	31
123	The Chief Scientist Office Cardiovascular and Pulmonary Imaging in SARS Coronavirus disease-19 (CISCO-19) study. Cardiovascular Research, 2020, 116, 2185-2196.	1.8	31
124	Unsupervised Inline Analysis of Cardiac Perfusion MRI. Lecture Notes in Computer Science, 2009, 12, 741-749.	1.0	31
125	Effectiveness of late gadolinium enhancement to improve outcomes prediction in patients referred for cardiovascular magnetic resonance after echocardiography. Journal of Cardiovascular Magnetic Resonance, 2013, 15, 6.	1.6	30
126	Mechanisms for overestimating acute myocardial infarct size with gadolinium-enhanced cardiovascular magnetic resonance imaging in humans: a quantitative and kinetic study. European Heart Journal Cardiovascular Imaging, 2015, 17, jev123.	0.5	30

#	Article	IF	CITATIONS
127	Assessment of Multivessel Coronary Artery Disease Using Cardiovascular Magnetic Resonance Pixelwise Quantitative Perfusion Mapping. JACC: Cardiovascular Imaging, 2020, 13, 2546-2557.	2.3	30
128	Real-time blood flow imaging using autocalibrated spiral sensitivity encoding. Magnetic Resonance in Medicine, 2005, 54, 1557-1561.	1.9	29
129	Free-breathing T2* mapping using respiratory motion corrected averaging. Journal of Cardiovascular Magnetic Resonance, 2015, 17, 3.	1.6	29
130	Clinical impact of cardiovascular magnetic resonance with optimized myocardial scar detection in patients with cardiac implantable devices. International Journal of Cardiology, 2019, 279, 72-78.	0.8	29
131	High Spatial Resolution Cardiovascular Magnetic Resonance at 7.0 Tesla in Patients with Hypertrophic Cardiomyopathy – First Experiences: Lesson Learned from 7.0 Tesla. PLoS ONE, 2016, 11, e0148066.	1.1	28
132	Acute changes in cardiac structural and tissue characterisation parameters following haemodialysis measured using cardiovascular magnetic resonance. Scientific Reports, 2019, 9, 1388.	1.6	27
133	Automatic inâ€line quantitative myocardial perfusion mapping: Processing algorithm and implementation. Magnetic Resonance in Medicine, 2020, 83, 712-730.	1.9	27
134	Method for functional MRI mapping of nonlinear response. NeuroImage, 2003, 19, 190-199.	2.1	26
135	Exploiting Quasiperiodicity in Motion Correction of Free-Breathing Myocardial Perfusion MRI. IEEE Transactions on Medical Imaging, 2010, 29, 1516-1527.	5.4	26
136	Infiltrated atrial fat characterizes underlying atrial fibrillation substrate in patients at risk as defined by the ARIC atrial fibrillation risk score. International Journal of Cardiology, 2014, 172, 196-201.	0.8	26
137	Myocardial extracellular volume fraction quantified by cardiovascular magnetic resonance is increased in hypertension and associated with left ventricular remodeling. European Radiology, 2017, 27, 4620-4630.	2.3	26
138	Inline perfusion mapping provides insights into the disease mechanism in hypertrophic cardiomyopathy. Heart, 2020, 106, 824-829.	1.2	26
139	Direct comparison of myocardial perfusion cardiovascular magnetic resonance sequences with parallel acquisition. Journal of Magnetic Resonance Imaging, 2007, 26, 1444-1451.	1.9	25
140	Characterization of T ₁ bias in skeletal muscle from fat in MOLLI and SASHA pulse sequences: Quantitative fatâ€fraction imaging with T ₁ mapping. Magnetic Resonance in Medicine, 2017, 77, 237-249.	1.9	25
141	Cardiovascular Determinants of Aerobic Exercise Capacity in Adults With Type 2 Diabetes. Diabetes Care, 2020, 43, 2248-2256.	4.3	25
142	A comparison of cine CMR imaging at 0.55 T and 1.5 T. Journal of Cardiovascular Magnetic Resonance, 2020, 22, 37.	1.6	25
143	T2* measurement during first-pass contrast-enhanced cardiac perfusion imaging. Magnetic Resonance in Medicine, 2006, 56, 1132-1134.	1.9	24
144	Improved workflow for quantification of left ventricular volumes and mass using free-breathing motion corrected cine imaging. Journal of Cardiovascular Magnetic Resonance, 2016, 18, 10.	1.6	24

#	Article	IF	CITATIONS
145	The relative contributions of myocardial perfusion, blood volume and extracellular volume to native T1 and native T2 at rest and during adenosine stress in normal physiology. Journal of Cardiovascular Magnetic Resonance, 2019, 21, 73.	1.6	24
146	Landmark Detection in Cardiac MRI by Using a Convolutional Neural Network. Radiology: Artificial Intelligence, 2021, 3, e200197.	3.0	24
147	Ultrafast Magnetic Resonance Imaging for Iron Quantification in Thalassemia Participants in the Developing World. Circulation, 2016, 134, 432-434.	1.6	23
148	T1 mapping performance and measurement repeatability: results from the multi-national T1 mapping standardization phantom program (T1MES). Journal of Cardiovascular Magnetic Resonance, 2020, 22, 31.	1.6	23
149	Motion-corrected free-breathing LGE delivers high quality imaging and reduces scan time by half: an independent validation study. International Journal of Cardiovascular Imaging, 2019, 35, 1893-1901.	0.7	22
150	Assessing for Cardiotoxicity from Metal-on-Metal Hip Implants with Advanced Multimodality Imaging Techniques. Journal of Bone and Joint Surgery - Series A, 2017, 99, 1827-1835.	1.4	21
151	Blood correction reduces variability and gender differences in native myocardial T1 values at 1.5ÂT cardiovascular magnetic resonance – a derivation/validation approach. Journal of Cardiovascular Magnetic Resonance, 2016, 19, 41.	1.6	21
152	Artifact suppression in imaging of myocardial infarction usingB1-weighted phased-array combined phase-sensitive inversion recovery. Magnetic Resonance in Medicine, 2004, 51, 408-412.	1.9	20
153	Quantification of Left Ventricular Function With Premature Ventricular Complexes Reveals Variable Hemodynamics. Circulation: Arrhythmia and Electrophysiology, 2016, 9, e003520.	2.1	20
154	Free-breathing motion-corrected late-gadolinium-enhancement imaging improves image quality in children. Pediatric Radiology, 2016, 46, 983-990.	1.1	20
155	Automated detection of left ventricle in arterial input function images for inline perfusion mapping using deep learning: A study of 15,000 patients. Magnetic Resonance in Medicine, 2020, 84, 2788-2800.	1.9	19
156	Cardiac Magnetic Resonance–Derived Extracellular Volume Mapping for the Quantification of Hepatic and Splenic Amyloid. Circulation: Cardiovascular Imaging, 2021, 14, CIRCIMAGING121012506.	1.3	19
157	Detection of Recent Myocardial Infarction Using Native T1 Mapping in a Swine Model: A Validation Study. Scientific Reports, 2018, 8, 7391.	1.6	18
158	Prognostic Value of Pulmonary Transit Time and Pulmonary Blood Volume Estimation Using Myocardial PerfusionÂCMR. JACC: Cardiovascular Imaging, 2021, 14, 2107-2119.	2.3	18
159	Increased myocardial extracellular volume in active idiopathic systemic capillary leak syndrome. Journal of Cardiovascular Magnetic Resonance, 2015, 17, 76.	1.6	17
160	Subclinical myocardial injury in patients with Facioscapulohumeral muscular dystrophy 1 and preserved ejection fraction – assessment by cardiovascular magnetic resonance. Journal of Cardiovascular Magnetic Resonance, 2019, 21, 25.	1.6	17
161	Low latency temporal filter design for real-time MRI using UNFOLD. Magnetic Resonance in Medicine, 2000, 44, 933-939.	1.9	16
162	Quantitative cardiovascular magnetic resonance myocardial perfusion mapping to assess hyperaemic response to adenosine stress. European Heart Journal Cardiovascular Imaging, 2021, 22, 273-281.	0.5	15

#	Article	IF	CITATIONS
163	Myocardial Perfusion Defects in Hypertrophic Cardiomyopathy Mutation Carriers. Journal of the American Heart Association, 2021, 10, e020227.	1.6	15
164	Acute Cardiac MRI Assessment of Radiofrequency Ablation Lesions for Pediatric Ventricular Arrhythmia: Feasibility and Clinical Correlation. Journal of Cardiovascular Electrophysiology, 2017, 28, 517-522.	0.8	14
165	Diffuse myocardial fibrosis among healthy pediatric heart transplant recipients: Correlation of histology, cardiovascular magnetic resonance, and clinical phenotype. Pediatric Transplantation, 2017, 21, e12986.	0.5	14
166	Temporal filtering effects in dynamic parallel MRI. Magnetic Resonance in Medicine, 2011, 66, 192-198.	1.9	13
167	Improved accuracy and precision with threeâ€parameter simultaneous myocardial T ₁ and T ₂ mapping using multiparametric SASHA. Magnetic Resonance in Medicine, 2022, 87, 2775-2791.	1.9	13
168	Late Anthracycline-Related Cardiotoxicity in Low-Risk Breast Cancer Patients. Journal of the American College of Cardiology, 2017, 69, 2573-2575.	1.2	12
169	Phenotyping hypertrophic cardiomyopathy using cardiac diffusion magnetic resonance imaging: the relationship between microvascular dysfunction and microstructural changes. European Heart Journal Cardiovascular Imaging, 2022, 23, 352-362.	0.5	12
170	Temporal and spatial characteristics of the area at risk investigated using computed tomography and T ₁ -weighted magnetic resonance imaging. European Heart Journal Cardiovascular Imaging, 2015, 16, 1232-1240.	0.5	11
171	A comparison of standard and high dose adenosine protocols in routine vasodilator stress cardiovascular magnetic resonance: dosage affects hyperaemic myocardial blood flow in patients with severe left ventricular systolic impairment. Journal of Cardiovascular Magnetic Resonance, 2021, 23. 37.	1.6	11
172	Freeâ€breathing simultaneous <i>T</i> ₁ , <i>T</i> ₂ , and <i>T</i> ₂ ^{â^—} quantification in the myocardium. Magnetic Resonance in Medicine, 2021, 86, 1226-1240.	1.9	11
173	Automated Inâ€Line Artificial Intelligence Measured Global Longitudinal Shortening and Mitral Annular Plane Systolic Excursion: Reproducibility and Prognostic Significance. Journal of the American Heart Association, 2022, 11, e023849.	1.6	11
174	Single heartbeat cardiac tagging for the evaluation of transient phenomena. Magnetic Resonance in Medicine, 2005, 54, 1455-1464.	1.9	10
175	HTGRAPPA: Realâ€ŧime <i>B</i> ₁ â€weighted image domain TGRAPPA reconstruction. Magnetic Resonance in Medicine, 2009, 61, 1425-1433.	1.9	10
176	Dark-Blood Late-Enhancement ImagingÂlmproves Detection of Myocardial Infarction. JACC: Cardiovascular Imaging, 2018, 11, 1770-1772.	2.3	10
177	Simultaneous 13N-Ammonia and gadolinium first-pass myocardial perfusion with quantitative hybrid PET-MR imaging: a phantom and clinical feasibility study. European Journal of Hybrid Imaging, 2019, 3, 15.	0.6	10
178	Quantitative Myocardial Perfusion Predicts Outcomes in Patients With Prior SurgicalÂRevascularization. Journal of the American College of Cardiology, 2022, 79, 1141-1151.	1.2	10
179	Phased array ghost elimination (PACE) for segmented SSFP imaging with interrupted steady-state. Magnetic Resonance in Medicine, 2002, 48, 1076-1080.	1.9	9
180	Number of Pâ€Wave Fragmentations on Pâ€SAECG Correlates with Infiltrated Atrial Fat. Annals of Noninvasive Electrocardiology, 2014, 19, 114-121.	0.5	9

#	Article	IF	CITATIONS
181	FLASH proton density imaging for improved surface coil intensity correction in quantitative and semi-quantitative SSFP perfusion cardiovascular magnetic resonance. Journal of Cardiovascular Magnetic Resonance, 2015, 17, 16.	1.6	9
182	Blood volume measurement using cardiovascular magnetic resonance and ferumoxytol: preclinical validation. Journal of Cardiovascular Magnetic Resonance, 2018, 20, 62.	1.6	9
183	The Effect of Blood Composition on T1ÂMapping. JACC: Cardiovascular Imaging, 2019, 12, 1888-1890.	2.3	9
184	Myocardial Perfusion Imaging After Severe COVID-19 Infection Demonstrates Regional Ischemia Rather Than Global Blood Flow Reduction. Frontiers in Cardiovascular Medicine, 2021, 8, 764599.	1.1	9
185	Noise propagation in region of interest measurements. Magnetic Resonance in Medicine, 2015, 73, 1300-1308.	1.9	8
186	Dark blood Late Gadolinium Enhancement improves conspicuity of ablation lesions. Journal of Cardiovascular Magnetic Resonance, 2016, 18, P211.	1.6	8
187	Improved Workflow for Quantification of Right Ventricular Volumes Using Free-Breathing Motion Corrected Cine Imaging. Pediatric Cardiology, 2019, 40, 79-88.	0.6	8
188	Non-invasive characterization of pleural and pericardial effusions using T1 mapping by magnetic resonance imaging. European Heart Journal Cardiovascular Imaging, 2022, 23, 1117-1126.	0.5	8
189	Simultaneous myocardial strain and darkâ€blood perfusion imaging using a displacementâ€encoded MRI pulse sequence. Magnetic Resonance in Medicine, 2010, 64, 787-798.	1.9	7
190	Bright-blood and dark-blood phase sensitive inversion recovery late gadolinium enhancement and T1 and T2 maps in a single free-breathing scan: an all-in-one approach. Journal of Cardiovascular Magnetic Resonance, 2021, 23, 126.	1.6	7
191	Coronary microvascular function and visceral adiposity in patients with normal body weight and type 2 diabetes. Obesity, 2022, 30, 1079-1090.	1.5	7
192	Distinct cardiovascular phenotypes are associated with prognosis in systemic sclerosis: a cardiovascular magnetic resonance study. European Heart Journal Cardiovascular Imaging, 2023, 24, 463-471.	0.5	7
193	Measurement of T1 Mapping in Patients With Cardiac Devices: Off-Resonance Error Extends Beyond Visual Artifact but Can Be Quantified and Corrected. Frontiers in Cardiovascular Medicine, 2021, 8, 631366.	1.1	6
194	Hypertrophic cardiomyopathy: insights from extracellular volume mapping. European Journal of Preventive Cardiology, 2022, 28, e39-e41.	0.8	6
195	Use of quantitative cardiovascular magnetic resonance myocardial perfusion mapping for characterization of ischemia in patients with left internal mammary coronary artery bypass grafts. Journal of Cardiovascular Magnetic Resonance, 2021, 23, 82.	1.6	6
196	The Interfield Strength Agreement of Left Ventricular Strain Measurements at 1. <scp>5ÂT</scp> and <scp>3ÂT</scp> Using Cardiac <scp>MRI</scp> Feature Tracking. Journal of Magnetic Resonance Imaging, 2023, 57, 1250-1261.	1.9	6
197	Hemodynamic Consequences of Hypertrophic Cardiomyopathy with Midventricular Obstruction: Apical Aneurysm and Thrombus Formation. Journal of General Practice (Los Angeles, Calif), 2014, 02, .	0.1	5
198	Free breathing myocardial perfusion data sets for performance analysis of motion compensation algorithms. GigaScience, 2014, 3, 23.	3.3	5

#	Article	IF	CITATIONS
199	Autoâ€calibration approach for k–t SENSE. Magnetic Resonance in Medicine, 2014, 71, 1123-1129.	1.9	5
200	Automated inline extracellular volume (ECV) mapping. Journal of Cardiovascular Magnetic Resonance, 2015, 17, W6.	1.6	5
201	Nonrigid Motion Compensation of Free Breathing Acquired Myocardial Perfusion Data. Informatik Aktuell, 2011, , 84-88.	0.4	5
202	Association of ambulatory blood pressure with coronary microvascular and cardiac dysfunction in asymptomatic type 2 diabetes. Cardiovascular Diabetology, 2022, 21, .	2.7	5
203	Improved image reconstruction incorporating non-rigid motion correction for cardiac MRI using BLADE acquisition. Journal of Cardiovascular Magnetic Resonance, 2009, 11, .	1.6	4
204	Edema by T2-weighted imaging in salvaged myocardium is extracellular, not intracellular. Journal of Cardiovascular Magnetic Resonance, 2011, 13, .	1.6	4
205	Method for calculating confidence intervals for phase contrast flow measurements. Journal of Cardiovascular Magnetic Resonance, 2014, 16, 46.	1.6	4
206	Detection of myocarditis using T 1 and ECV mapping is not improved by early compared to late post ontrast imaging. Clinical Physiology and Functional Imaging, 2019, 39, 384-392.	0.5	4
207	Evaluation of Hepatic Iron Overload Using a Contemporary 0. <scp>55 T MRI</scp> System. Journal of Magnetic Resonance Imaging, 2022, 55, 1855-1863.	1.9	4
208	Diffusely Increased Myocardial Extracellular Volume With or Without Focal Late Gadolinium Enhancement. Journal of Thoracic Imaging, 2022, 37, 17-25.	0.8	4
209	Study protocol: MyoFit46—the cardiac sub-study of the MRC National Survey of Health and Development. BMC Cardiovascular Disorders, 2022, 22, 140.	0.7	4
210	Real time high spatial-temporal resolution flow imaging with spiral MRI using auto-calibrated SENSE. , 2004, 2004, 1914-7.		3
211	Synthetic phase sensitive inversion recovery late gadolinium enhancement from post-contrast T1-mapping shows excellent agreement with conventional PSIR-LGE for diagnosing myocardial scar. Journal of Cardiovascular Magnetic Resonance, 2014, 16, P213.	1.6	3
212	Variability of T1 in purpose recruited normal volunteers and patients as a function of shim (B0), flip angle (B1) and myocardial sector at 3T. Journal of Cardiovascular Magnetic Resonance, 2015, 17, P5.	1.6	3
213	Optimized saturation pulse rrains for SASHA T1 mapping at 3T. Journal of Cardiovascular Magnetic Resonance, 2015, 17, W20.	1.6	3
214	Progressive myocardial injury in myotonic dystrophy type II and facioscapulohumeral muscular dystrophy 1: a cardiovascular magnetic resonance follow-up study. Journal of Cardiovascular Magnetic Resonance, 2021, 23, 130.	1.6	3
215	On Breathing Motion Compensation in Myocardial Perfusion Imaging. , 2010, , .		2
216	Coronary MRA at 3 T using 3d multi-interleaved multi-echo acquisition with varpro fat-water separation. Journal of Cardiovascular Magnetic Resonance, 2010, 12, .	1.6	2

#	Article	IF	CITATIONS
217	Motion correction for myocardial T1 mapping using image registration with synthetic image estimation. Magnetic Resonance in Medicine, 2012, 67, spcone.	1.9	2
218	Accelerating Cardiovascular Magnetic Resonance Imaging: Signal Processing Meets Nuclear Spins [Life Sciences]. IEEE Signal Processing Magazine, 2014, 31, 138-143.	4.6	2
219	Validation of cardiac magnetic-resonance-derived left ventricular strain measurements from free-breathing motion-corrected cine imaging. Pediatric Radiology, 2019, 49, 68-75.	1.1	2
220	Clinical associations with stage B heart failure in adults with type 2 diabetes. Therapeutic Advances in Endocrinology and Metabolism, 2021, 12, 204201882110301.	1.4	2
221	Automatic in-plane rotation for doubly-oblique cardiac imaging. Journal of Magnetic Resonance Imaging, 2003, 18, 612-615.	1.9	1
222	Interrogation of the infarcted and salvaged myocardium using multi-parametric mapping cardiovascular magnetic resonance in reperfused ST-segment elevation myocardial infarction patients. Scientific Reports, 2019, 9, 9056.	1.6	1
223	A framework for constraining image SNR loss due to MR raw data compression. Magnetic Resonance Materials in Physics, Biology, and Medicine, 2019, 32, 213-225.	1.1	1
224	Effective Study: Development and Application of a Questionâ€Driven, Timeâ€Effective Cardiac Magnetic Resonance Scanning Protocol. Journal of the American Heart Association, 2022, 11, e022605.	1.6	1
225	Variability of perfusion dark rim artifacts due to Gibbs ringing. Journal of Cardiovascular Magnetic Resonance, 2009, 11, .	1.6	0
226	Cardiac involvement of the systemic disorder myotonic dystrophy type II - detection by CMR. Journal of Cardiovascular Magnetic Resonance, 2014, 16, P390.	1.6	0
227	Cardiac involvement of myotonic dystrophy type II in patients with preserved ejection fraction - Detection by CMR. Journal of Cardiovascular Magnetic Resonance, 2015, 17, P315.	1.6	0
228	Recurrent acute pericarditis diagnosed by extra-cellular volume maps. European Heart Journal, 2021, , .	1.0	0
229	Parallelized Hybrid TGRAPPA Reconstruction for Real-Time Interactive MRI. Lecture Notes in Computer Science, 2008, 11, 163-170.	1.0	0
230	Techniques for T1, T2, and Extracellular Volume Mapping. , 2019, , 15-26.e2.		0